

## Probing Three-dimensional Chiral Domain Walls in Polar Vortices

Sandhya Susarla<sup>1</sup>, Shanglin Hsu<sup>1</sup>, Piush Behera<sup>1,2,3</sup>, Benjamin Savitzky<sup>1</sup>, Sujit Das<sup>1</sup>, Peter Ercius<sup>1</sup>, Colin Ophus<sup>1</sup>, Ramamoorthy Ramesh<sup>1,2,3,4</sup>

<sup>1</sup> National Center for Electron Microscopy, Lawrence Berkeley National Laboratory, Berkeley, CA,

<sup>2</sup> Materials Sciences Division, Lawrence Berkeley Laboratory, Berkeley CA

<sup>3</sup> Department of Materials Science & Engineering, University of California, Berkeley, CA

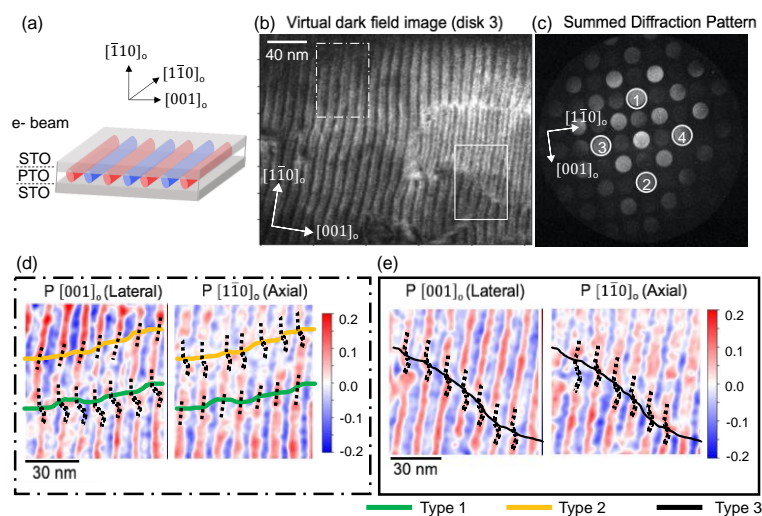
<sup>4</sup> Department of Physics, University of California, Berkeley Berkeley, CA

Over the past few years, novel polarization textures have been engineered in oxide superlattices using the interactions of elastic, electrostatic and gradient energies.[1] Surprisingly, emergent chirality is observed in one such topological texture i.e. polar vortices in  $\text{PbTiO}_3/\text{SrTiO}_3$  superlattices.[2–4] There are equal mixtures of left-handed and right-handed domains in superlattices. Perhaps, the most interesting part is how do these left/right-handed domains evolve at the nanoscale. What are the local physical parameters that are at play when handedness in local domains change? All these questions are critical for understanding the mechanism and dynamics of electrically switchable chiral devices. Quantitative scanning transmission electron microscopy (STEM) techniques like four-dimensional (4D) STEM can precisely measure strain, and thus polarization in ferroelectric oxides due to breaking of Friedel's Law.[5] This makes 4D-STEM a unique tool to probe polarization in three-dimensions and understand emergent chirality in polarization vortices.

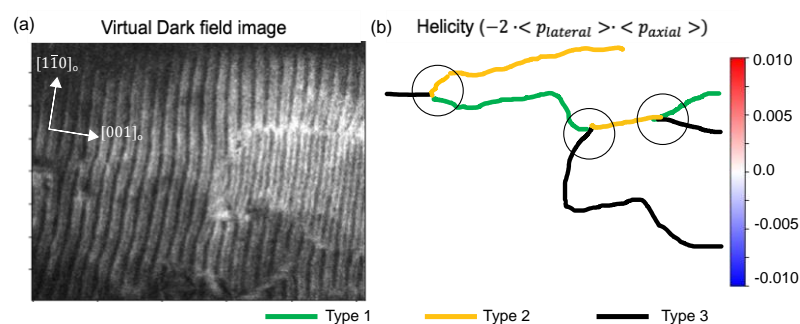
Herein, we image the three-dimensional chiral domain walls in polar vortices by 4D-STEM strain mapping using a K3 direct electron detector to understand the nano-scale nature of chirality in these systems. We observe the presence of both chiral and achiral boundaries in the system and find that achiral/chiral domains are sensitive to changes in local axial and lateral polarization across the boundaries. We have also discovered new triple point topologies in the system where the achiral and chiral boundaries meet.

Figure 1(a) shows the sample geometry of  $\text{PbTiO}_3/\text{SrTiO}_3$  used for 4D-STEM mapping. Figure 1(b) shows the virtual dark-field field image from the  $[2\bar{1}0]_o$  diffraction disk. The corresponding polarization maps were obtained by normalized intensity difference between the two opposite Friedel pair disks as shown in Figure 1(c). The zoomed images of the axial and lateral polarization maps along in Figure 1(d,e) show three types of domain walls identified as Type 1: anti-parallel lateral component, Type 2: anti-parallel axial component and Type 3: anti-parallel lateral and axial component.

Chirality in these topologies can be mathematically quantified as helicity which is dependent on both the lateral and axial polarization. We use the lateral and axial polarization maps to determine the helicity in the system and identified two types chiral domain walls (Type 1 and Type 2) and an achiral domain wall (Type 3). We also identified triple points in the system where chiral and achiral boundaries meet. The ordering of these triple points could be critical to control the dynamics of electrical switching devices built using chirality switching phenomenon.[6]



**Figure 1: Identification of polarization using 4D-STEM mapping.** (a) Schematic showing the e- beam scanned in 4D STEM mode across the vortex sample prepared with an in-plane geometry. (b) Virtual dark field image obtained via integrating the intensity of disk 3 ( $[2\bar{1}0]_o$ ) labeled in the mean diffraction pattern in (c). (d) Lateral ( $P[001]_o$ ) and (e) axial ( $P[1\bar{1}0]_o$ ) polarization produced by subtracting the normalized intensities of opposite Friedel pairs disks (1-2 and 3-4, respectively) as labeled in (c).



**Figure 2: Identification of triple point topologies and chirality boundaries.** (a) Virtual dark field image formed from the  $[2\bar{1}0]_o$  diffraction disk. (b) Corresponding helicity map showing left and right handed domains separated by type 1 (green) and type 2 (orange) domain walls. Additionally, achiral domain boundaries (black line) also exist. The resultant triple point topologies formed due to the co-existence of chiral and achiral boundaries are shown circled.

boundaries (black line) also exist. The resultant triple point topologies formed due to the co-existence of chiral and achiral boundaries are shown circled.

## References:

- [1] S. Das et. al., *APL Mater.* **6**, 100901 (2018).
- [2] A. K. Yadav et. al., *Nature* **530**, 198 (2016).
- [3] P. Shafer et. al., *Proc. Natl. Acad. Sci. U. S. A* **115**, 915 (2018).
- [4] P. Behera et al, *Sci. Adv.* **8**, eabj8030 (2022).
- [5] C. Ophus, *Microsc. Microanal.* **25**, 563 (2019).
- [6] The electron microscopy experiments were performed at the Molecular Foundry, Lawrence Berkeley National Laboratory, which is supported by the U.S. Department of Energy under contract no. DE-AC02-05CH11231. S.S. is supported by the DOE BES program on Quantum Materials.